A diagram of the minimum necessary internal force required to resist external forces on two-point-grasped objects in two-dimensional space

Satoshi Ito, Kohta Tanaka and Minoru Sasaki

Link to this article: http://journals.cambridge.org/abstract_S0263574711001135

How to cite this article:
Satoshi Ito, Kohta Tanaka and Minoru Sasaki (2012). A diagram of the minimum necessary internal force required to resist external forces on two-point-grasped objects in two-dimensional space. Robotica, 30, pp 857-864 doi:10.1017/S0263574711001135

Request Permissions : Click here

A diagram of the minimum necessary internal force required to resist external forces on two-point-grasped objects in two-dimensional space

Satoshi Ito*, Kohta Tanaka and Minoru Sasaki

Faculty of Engineering, Gifu University, Yanagido 1-1, Gifu 501-1193, Japan

SUMMARY
This paper considers the magnitude of the gripping power, i.e., the internal force that depends on the grasping posture or object orientation in a two-dimensional grasp by two contact points with friction. Expressing the effect of variations in the object posture as the direction of an external force, we propose an "internal force diagram." The internal force necessary to create a statically stable grasp is depicted in the object coordinate frame. Then, a polar coordinate system is introduced in which the orientation represents the direction of the external force, while the distance from the origin represents the minimum necessary internal force. We demonstrate a method based on friction cone configurations to manually draw the internal force diagram, using only a ruler and a compass. The validity of this drawing method is confirmed by a comparison with computer-generated plots. Finally, the characteristics of the internal force diagram are discussed.

KEYWORDS: Grasping; Gripping power; Diagram expression; Internal force magnitude; External force direction.

1. Introduction
Grasping contains many redundancy problems.[1,2] Many studies have focused on the selection of contact points or joint torques,[3–7] and many solution approaches have been proposed.[8–12]

This paper deals with the problem of redundancy of gripping power. The problem is that the gripping power necessary to create a statically stable grasp depends on the grasping posture, or the object orientation. A typical case is shown in Fig. 1. Although no other joint torques are affected by the object orientation, the gripping power varies with the object orientation. Thus, it is difficult to determine the object postures that are easy or difficult to grasp, and how much gripping power is necessary or sufficient when the object posture changes. To solve these problems, the magnitude of the gripping power, i.e., the internal force, is investigated when the external force being exerted on the Center of Mass (CoM) of the object varies in direction. Such an external force

can represent a change in the object posture by considering gravity as the external force.

We have modeled the situation in Fig. 1 as a two-dimensional (2D) grasp by two contact points with friction, and have analytically modeled an optimal object in the sense that the least contact forces are required.[13–15] However, the problem of finding an object orientation that requires the maximum internal force cannot be solved analytically because of the complexity of the trigonometric calculations. This is the reason we take a graphical approach in this paper. The relative magnitude of the internal force required to create a statically stable grasp is depicted in the object coordinate frame using a polar graph whose orientation represents the external force direction, including the gravity. Nakamura *et al.*[16,17] proposed the concept of a marginal external force for representing a power grasp in 3D space. Nakamura *et al.* defined the marginal external force as an external force that exists when a slip at the contact points is about to occur. Conversely, this paper gives the necessary internal force that can balance the effect of a given external force, although the application is limited to a 2D grasp with two contact points. Such an inverse approach is important for robotic designs.

This paper is organized as follows. Section 2 describes some assumptions, defines the problem, and gives a solution by equations. This solution representing the relation between the magnitude of the internal force and the direction of the external force is illustrated as a diagram, i.e., a graph in the polar coordinate system in Section 3. Here, a method to draw this diagram is proposed. This method is completely graphical, i.e., does not need any calculations. In Section 4, the validity of our proposed method will be confirmed using some examples of typical diagrams. Properties of this kind of diagram are discussed in Section 5, and finally this paper is concluded in Section 6.

2. Problem Formulation and Solution

2.1. Assumptions and problem
In order to facilitate our mathematical analysis, we assume the following:

- An object is grasped at two contact points and resides in 2D space.
- The object is convex and rigid.

* Corresponding author. Email: satoshi@gifu-u.ac.jp
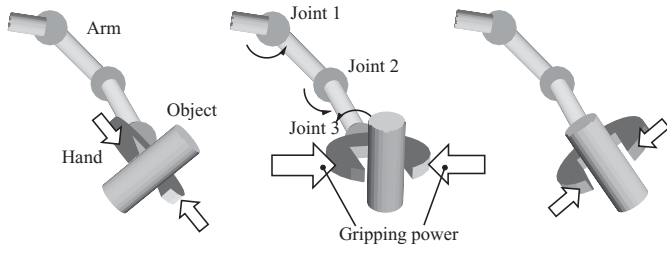
Fig. 1. Gripping power varying with object orientation.
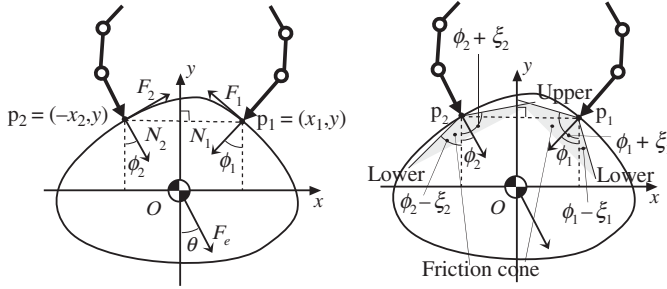
Fig. 2. Variables and coordinate frame.

- The shape of the object is smooth at the contact points.
- The contacts are point contact with friction.
- An external force, which may include the gravitational force, is exerted at the CoM of the object.

In order to grasp the object stably, a necessary magnitude of the internal force varies with the direction of the external force. So, our problem is to associate the magnitude of the smallest internal force for stable grasp with respect to the direction of the external force: Smaller internal force allows us to maintain an object's posture more efficiently with less gripping power.

2.2. Formulation

2.2.1. Coordinate frame. The object coordinate frame is defined with the origin at the object's CoM with the y-axis orthogonal to the line connecting the two contact points as shown in Fig. 2. With this object coordinate frame, the external force exerted to the CoM of the object is directed by angle θ from the negative y-axis.

In the object coordinate frame, the coordinates of the two contact points are denoted by $p_1 = (x_1, y)$ and $p_2 = (-x_2, y)(\neq p_1)$, and the normals to the edge of the object at these contact points make angles ϕ_1 (CW) and ϕ_2 (CCW) from the negative y-axis. Here, $x_1 > 0$, $x_2 > 0$, $y \geq 0$, and $0 < \phi_1 \leq \pi$, $0 < \phi_2 \leq \pi$.

2.2.2. Contact point conditions. If the friction cone of each contact point contains the other contact point, then the object can be grasped by these two contact points,[1] as shown in the right side of Fig. 2. This condition can be described with the following inequalities:

$$-\frac{\pi}{2} < \phi_i - \xi_i < \frac{\pi}{2} < \phi_i + \xi_i < \frac{3\pi}{2} \quad (i = 1, 2). \quad (1)$$

Here, ξ_i $(0 < \xi_i < \pi/2)$ is an apex angle of the friction cone. This comes from the conditions that the segment connecting

two contact points is under the upper lateral surface and over the lower lateral surface of both friction cones. These conditions actually restrict the range of ξ_i, i.e., provide the lower limits of ξ_i in grasping this object at the points p_1 and p_2.

2.2.3. Force balance conditions. N_i and F_i $(i = 1, 2)$ are defined as the normal and tangential component of the contact force at each contact point. For stable grasp, not only must the forces but also the moments be balanced among the contact forces and the external force. This condition can be stated as

$$L\boldsymbol{F} = \boldsymbol{M}, \quad (2)$$

where the contact force vector $\boldsymbol{F}$ and the external force vector $\boldsymbol{M}$ are defined as follows:

$$\boldsymbol{F} = [\, N_1 \; F_1 \; N_2 \; F_2 \,]^T, \quad (3)$$

$$\boldsymbol{M} = [\, -F_e s \;\; F_e c \;\; 0 \,]^T. \quad (4)$$

Here, F_e is magnitude of the external force, $s = \sin\theta$, and $c = \cos\theta$. The matrix L is called the grasp matrix, and defined as

$$L = \begin{bmatrix} -s_1 & -c_1 & s_2 & c_2 \\ -c_1 & s_1 & -c_2 & s_2 \\ L_{31} & L_{32} & L_{33} & L_{34} \end{bmatrix}, \quad (5)$$

$$L_{31} = -c_1 x_1 + s_1 y, \;\; L_{32} = +s_1 x_1 + c_1 y,$$

$$L_{33} = +c_2 x_2 - s_2 y, \;\; L_{34} = -s_2 x_2 - c_2 y.$$

Here, $s_i = \sin\phi_i$, and $c_i = \cos\phi_i$.

2.2.4. Contact force conditions. The normal force works so as to only push the object:

$$N_1 > 0, \quad (6)$$

$$N_2 > 0. \quad (7)$$

In addition, the vector of the contact force must be included within the friction cone. In other words, to keep contact without slipping, the tangential force must never exceed the maximal static friction force. This holds if $|F_i| < \mu_i N_i$, where μ_i is the friction coefficient at point p_i. This condition can be decomposed to the following four inequalities:

$$\mu_1 N_1 - F_1 > 0, \quad (8)$$

$$\mu_2 N_2 - F_2 > 0, \quad (9)$$

$$\mu_1 N_1 + F_1 > 0, \quad (10)$$

$$\mu_2 N_2 + F_2 > 0. \quad (11)$$

Generally, if the above four inequalities hold, then Eqs. (6) and (7) are automatically satisfied. Thus, Eqs. (8)–(11) are considered as contact force conditions throughout this paper.

2.2.5. Problem description. Now, the problem can be mathematically described as follows:

Definition 1. *Under the contact point conditions (1), the force balance condition (2) and the contact force conditions (8)–(11) investigate the relation between the direction of the external force θ and the magnitude of the internal force required to create a stable grasp with friction.*

Instead of the actual magnitude of the internal force, a scaled parameter is introduced in the next section.

2.3. Solution
First of all, equality (2) is solved. This solution can be represented as

$$\boldsymbol{F} = L^{\dagger}\boldsymbol{M} + (I - L^{\dagger}L)\boldsymbol{\kappa}, \tag{12}$$

where $L^{\dagger}$ is a pseudo-inverse matrix of L that can be calculated as $L^{\dagger} = L^T(LL^T)^{-1}$, and $\boldsymbol{\kappa} \in R^4$ is an arbitrary vector. Let the first term of the right-hand side be $\boldsymbol{F}_T$. Then $\boldsymbol{F}_T$ is given from the definition as follows:

$$\boldsymbol{F}_T = \frac{F_e}{2(x_1 + x_2)} \begin{bmatrix} (x_1 + x_2)s_1 s + 2(ys - x_2 c)c_1 \\ (x_1 + x_2)c_1 s - 2(ys - x_2 c)s_1 \\ -(x_1 + x_2)s_2 s - 2(ys + x_1 c)c_2 \\ -(x_1 + x_2)c_2 s + 2(ys + x_1 c)s_2 \end{bmatrix}. \tag{13}$$

On the other hand, the second term of the right-hand side is written as follows:

$$(I - L^{\dagger}L)\boldsymbol{\kappa} = k\boldsymbol{F}_N. \tag{14}$$

Here,

$$\boldsymbol{F}_N = \frac{F_e}{2(x_1 + x_2)} \begin{bmatrix} 2s_1 \\ 2c_1 \\ 2s_2 \\ 2c_2 \end{bmatrix}, \tag{15}$$

and k is a scalar value that is proportional to the magnitude of the internal force exerted to the object. As the contact forces are repulsive, k should not be negative. In summary, the solution of equality (2) becomes

$$\boldsymbol{F} = \boldsymbol{F}_T + k\boldsymbol{F}_N. \tag{16}$$

Instead of the actual magnitude of the internal force, i.e., F_{int}, the actual magnitude of the scaled parameter k is considered. The relation between F_{int} and k is

$$F_{\text{int}} = k/(x_1 + x_2) \cdot F_e. \tag{17}$$

Namely, F_{int} is proportional to F_e, the magnitude of external force being exerted to the CoM of the object. To calculate F_{int}, k as well as the inverse of the distance between two contact points must be multiplied to F_e.

Next, among the solutions, relation (16), the one satisfying each inequality conditions (8)–(11), is considered. A large k generically satisfies all these inequalities. Thus, the lower limit of k is calculated. Now, let $k_n(\theta)$ ($n = 1, \ldots, 4$) be the lower limit that satisfy each inequality condition (8)–(11). These are given as follows from relation (16) substituted by Eqs. (13) and (15):

$$k_1(\theta) = -\frac{x_1 + x_2}{2}s + (x_2 c - ys) \cdot \frac{c_1 \mu_1 + s_1}{s_1 \mu_1 - c_1}$$
$$= -\frac{x_1 + x_2}{2}s - (x_2 c - ys)\tan(\phi_1 + \xi_1), \tag{18}$$

$$k_2(\theta) = +\frac{x_1 + x_2}{2}s + (x_1 c + ys) \cdot \frac{c_2 \mu_2 + s_2}{s_2 \mu_2 - c_2}$$
$$= +\frac{x_1 + x_2}{2}s - (x_1 c + ys)\tan(\phi_2 + \xi_2), \tag{19}$$

$$k_3(\theta) = -\frac{x_1 + x_2}{2}s + (x_2 c - ys) \cdot \frac{c_1 \mu_1 - s_1}{s_1 \mu_1 + c_1}$$
$$= -\frac{x_1 + x_2}{2}s - (x_2 c - ys)\tan(\phi_1 - \xi_1), \tag{20}$$

$$k_4(\theta) = +\frac{x_1 + x_2}{2}s + (x_1 c + ys) \cdot \frac{c_2 \mu_2 - s_2}{s_2 \mu_2 + c_2}$$
$$= +\frac{x_1 + x_2}{2}s - (x_1 c + ys)\tan(\phi_2 - \xi_2). \tag{21}$$

In the above calculations, the relation between the apex angle ξ_i and the friction coefficient μ_i is

$$\tan \xi_i = \mu_i \tag{22}$$

as well as the following one was applied,

$$-\frac{c_i \mu_i \pm s_i}{s_i \mu_i \mp c_i} = \frac{s_i \pm c_i \mu_i}{c_i \mp s_i \mu_i} = \frac{\frac{s_i}{c_i} \pm \mu_i}{1 \mp \frac{s_i}{c_i}\mu_i}$$
$$= \frac{\tan \phi_i \pm \tan \xi_i}{1 \mp \tan \phi_i \tan \xi_i} = \tan(\phi_i \pm \xi_i), \tag{23}$$

$k = k(\theta)$ that enables the grasp must be greater than all the $k_n(\theta)$,

$$k(\theta) > k_n(\theta)\,(n = 1, \ldots, 4). \tag{24}$$

Thus, the smallest internal forces required for the stable grasp, i.e., $k_{\text{grasp}}(\theta)$, is obtained by selecting the maximum $k_n(\theta)\,(n = 1, \ldots, 4)$ at each θ within non-negative range:

$$k_{\text{grasp}}(\theta) = \max\{k_1(\theta), k_2(\theta), k_3(\theta), k_4(\theta), 0\}. \tag{25}$$

This nonlinear, almost piecewise sinusoidal function, $k_{\text{grasp}}(\theta)$, provides us necessary informations of internal force through relation (17).

3. Graphical Expression of Necessary Internal Force

3.1. Motivations
In the previous paper,[15] we analyzed the minimum points of the internal force $k_{\text{grasp}}(\theta)$ and discussed their physical meanings. However, it is difficult to mathematically explain those of the maximum point of $k_{\text{grasp}}(\theta)$, i.e., the direction
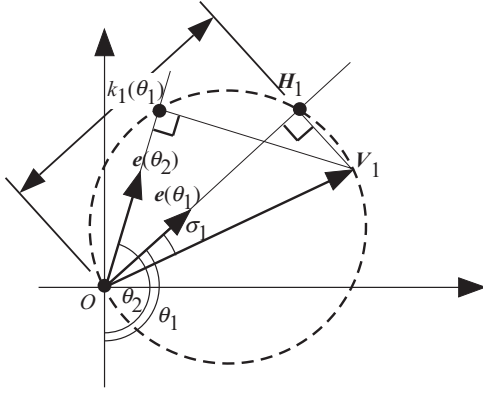
Fig. 3. Inner product.

of the external force that requires the largest internal force. That is why we try to draw the relative magnitude of the necessary internal forces in the object coordinate frame, such as Fig. 7, with respect to the direction of external forces. Here, the relation between external force direction and internal force magnitude is represented using the polar coordinate system whose origin is set to the CoM of the object. This graphical expression, i.e., we call here "internal force diagram," visually shows the minimum necessary internal force when the direction of the external force varies.

3.2. Method
The internal force diagram is initiated by drawing each $k_n(\theta)$ ($n = 1, 2, 3, 4$) in Eqs. (18)–(21) in the object coordinate frame.

Let us take $k_1(\theta)$ as an example. The unit vector representing the direction of the external force is defined as

$$e(\theta) = \begin{bmatrix} \sin\theta & -\cos\theta \end{bmatrix}^T. \tag{26}$$

$k_1(\theta)$ in Eq. (18) can be represented using the inner product with e as follows:

$$
\begin{aligned}
k_1(\theta) &= \left(-\frac{x_1 + x_2}{2} + y\tan(\phi_1 + \xi_1) \right) \sin\theta \\
&\quad - (x_2 \tan(\phi_1 + \xi_1)) \cos\theta \\
&= S_1 \sin\theta - C_1 \cos\theta \\
&= V_1 \cdot e(\theta),
\end{aligned}
\tag{27}
$$

where

$$S_1 = -\frac{x_1 + x_2}{2} + y\tan(\phi_1 + \xi_1), \tag{28}$$

$$C_1 = x_2 \tan(\phi_1 + \xi_1), \tag{29}$$

$$V_1 = \begin{bmatrix} S_1 & C_1 \end{bmatrix}^T. \tag{30}$$

Here, plot the magnitude of $k_1(\theta)$ in the direction of $e(\theta)$. This is equivalent to drawing it in the polar system. Since $e(\theta)$ is a unit vector, this is achieved by plotting a perpendicular drawn from V_1 to $e(\theta)$, labeled as H_1, as shown in Fig. 3.

This is because

$$
\begin{aligned}
k_1(\theta) &= V_1 \cdot e(\theta) \\
&= |V_1||e(\theta)| \cos\sigma_1 \\
&= |V_1| \cos\sigma_1 \\
&= \overline{OH_1},
\end{aligned}
\tag{31}
$$

where σ_1 is the angle between V_1 and $e(\theta)$.

Now, change the external force orientation θ. According to the theorem of the inscribed angle, point H_1 moves on the circle whose diameter is V_1.

In an analogous way, draw $k_2(\theta)$, $k_3(\theta)$, and $k_4(\theta)$ in the object coordinate frame. Each of these involves a circle of diameter V_n, as shown in the following equations:

$$k_n(\theta) = V_n \cdot e \quad (n = 2, 3, 4), \tag{32}$$

where

$$V_n = \begin{bmatrix} S_n & C_n \end{bmatrix}^T, \tag{33}$$

$$S_2 = +\frac{x_1 + x_2}{2} - y\tan(\phi_2 + \xi_2), \tag{34}$$

$$C_2 = x_1 \tan(\phi_2 + \xi_2), \tag{35}$$

$$S_3 = -\frac{x_1 + x_2}{2} + y\tan(\phi_1 - \xi_1), \tag{36}$$

$$C_3 = x_2 \tan(\phi_1 - \xi_1), \tag{37}$$

$$S_4 = +\frac{x_1 + x_2}{2} - y\tan(\phi_2 - \xi_2), \tag{38}$$

$$C_4 = x_1 \tan(\phi_2 - \xi_2). \tag{39}$$

Finally, k_{grasp} is obtained by selecting the largest k_n, in other words, the outermost circle in all radial directions.

3.3. Manual drawing steps
Vector V_n ($n = 1, \ldots, 4$) can be drawn if information about the corresponding friction cones (i.e., position and angle of the apex) is known. The steps for V_1 are listed below and shown in Fig. 4(a).

Before that, P_{1x} and P_{2x} are defined as the intersections of perpendiculars dropped from P_1 and P_2 to the x-axis. In addition, the midpoint of the segment connecting them is labeled as O_M.

Manual drawing step of V_1 (see Fig. 4(a))

(1) Extend the upper side of the friction cone at P_1 until it intersects the x-axis and label the intersection as X_1. Then, $\overline{O_M X_1}$ is equal to $-S_1$ in Eq. (28).
(2) Draw a perpendicular from P_{2x} to the upper side of the friction cone at P_1 (the line going through P_1 and X_1) and label its intersection with the y-axis as Y_1. Then, $\overline{OY_1}$ is equal to $-C_1$ in Eq. (29).
(3) Plot the point $(-\overline{O_M X_1}, -\overline{OY_1})$ and define it as V_1.

The other points V_n ($n = 2, 3, 4$) are plotted in a similar way.
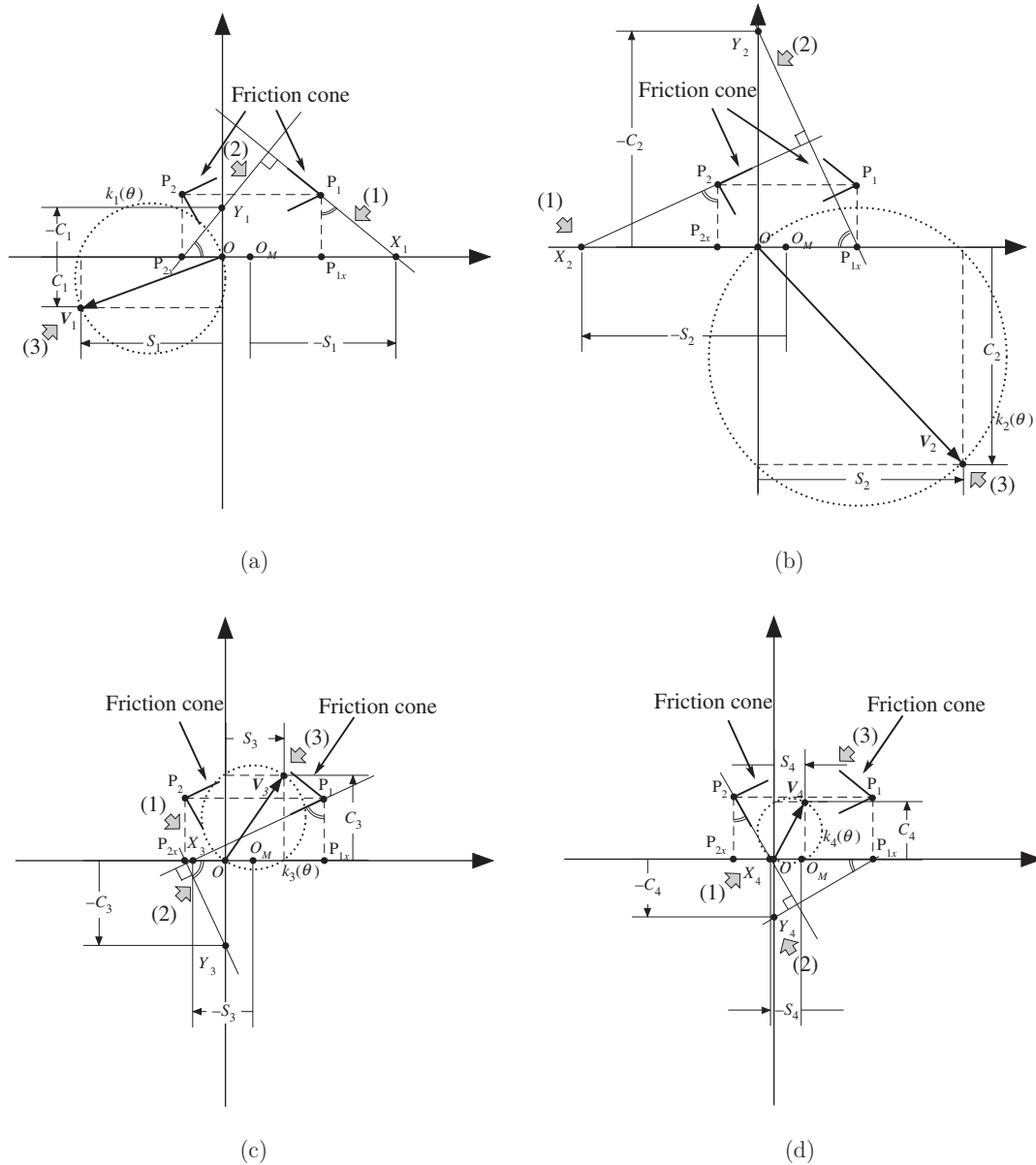
Fig. 4. Drawing steps of each vector V_i ($i = 1, \ldots, 4$). (a) Vector V_1; (b) vector V_2; (c) vector V_3; and (d) vector V_4.

Manual drawing step of V_2 (see Fig. 4(b))

(1) Extend the upper side of the friction cone at P_2 until it intersects the x-axis and label the intersection as X_2. Then, $\overline{O_M X_2}$ is equal to $-S_2$ in Eq. (34).
(2) Draw a perpendicular from P_{1x} to the upper side of the friction cone at P_2 (the line going through P_2 and X_2) and label its intersection with the y-axis as Y_2. Then, $\overline{OY_2}$ is equal to $-C_2$ in Eq. (35).
(3) Plot the point $(-\overline{O_M X_2}, -\overline{OY_2})$ and define it as V_2.

Manual drawing step of V_3 (see Fig. 4(c))

(1) Extend the lower side of the friction cone at P_1 until it intersects the x-axis and label the intersection as X_3. Then, $\overline{O_M X_3}$ is equal to $-S_3$ in Eq. (36).

(2) Draw a perpendicular from P_{2x} to the lower side of the friction cone at P_1 (the line going through P_1 and X_3) and label its intersection with the y-axis as Y_3. Then, $\overline{OY_3}$ is equal to $-C_3$ in Eq. (37).
(3) Plot the point $(-\overline{O_M X_3}, -\overline{OY_3})$ and define it as V_3.

Manual drawing step of V_4 (see Fig. 4(d))

(1) Extend the lower side of the friction cone at P_2 until it intersects the x-axis and label the intersection as X_4. Then, $\overline{O_M X_4}$ is equal to $-S_4$ in Eq. (38).
(2) Draw a perpendicular from P_{1x} to the lower side of the friction cone at P_2 (the line going through P_2 and X_4) and label its intersection with the y-axis as Y_4. Then, $\overline{OY_4}$ is equal to $-C_4$ in Eq. (39).
(3) Plot the point $(-\overline{O_M X_4}, -\overline{OY_4})$ and define it as V_4.
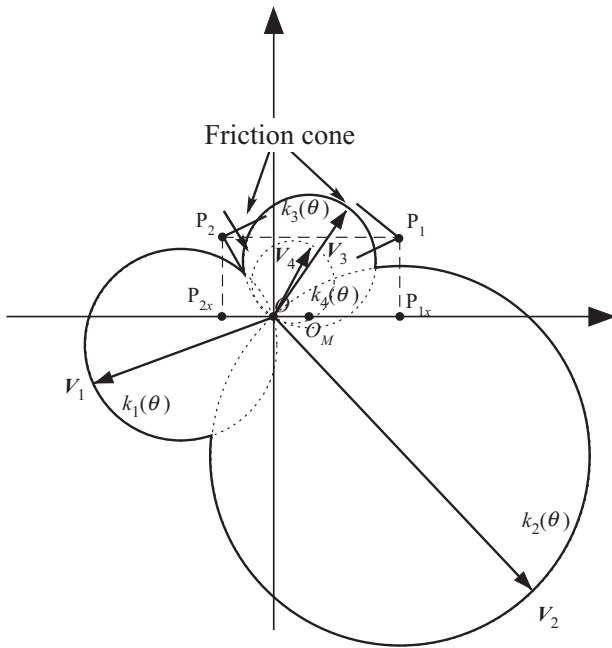
Fig. 5. Diagram of the minimal internal force in the polar coordinate system.

The proof of the equalities $\overline{O_M X_n} = -S_n$ and $\overline{OY_n} = -C_n (n = 1, \ldots, 4)$ will be shown in Appendix.

Outside extraction of four circles

After that, draw the circles whose diameters are V_n ($n = 1, \ldots, 4$) respectively, and extract the outside of these circles. The final diagram is illustrated in Fig. 5. This diagram is drawable with compass and ruler without scales.

4. Examples

4.1. Validity of manual drawing

In order to verify the validity of the manually drawn diagram, we examine a typical example, a circular object grasp, comparing drawings done by hand with plots done by computer. Parameters are $P_1 = (\sqrt{3}/2, 1/2)$, $P_2 = (-\sqrt{3}/2, 1/2)$, $\phi_1 = \phi_2 = \pi/3$, $\xi_1 = \pi/4$, $\xi_2 = \pi/3$. The results are shown in Fig. 6, where 6(a) is drawn according to our method and 6(b) is the result of computer calculation. The two figures are identical, indicating that our method is valid.

4.2. Variety of the diagram in shape

Next, we examine the variation of the diagram in shape using a rectangular object grasp by changing the position of the contact points and friction coefficients. Three cases are drawn in Fig. 7. Parameters are set as shown in Table I. The directions of vectors V_3 and V_4 are switched in case (a) and case (b). In case (c), both V_3 and V_4 face to the right.

5. Discussion

The internal force required to create a statically stable grasp changes with respect to the direction of the external
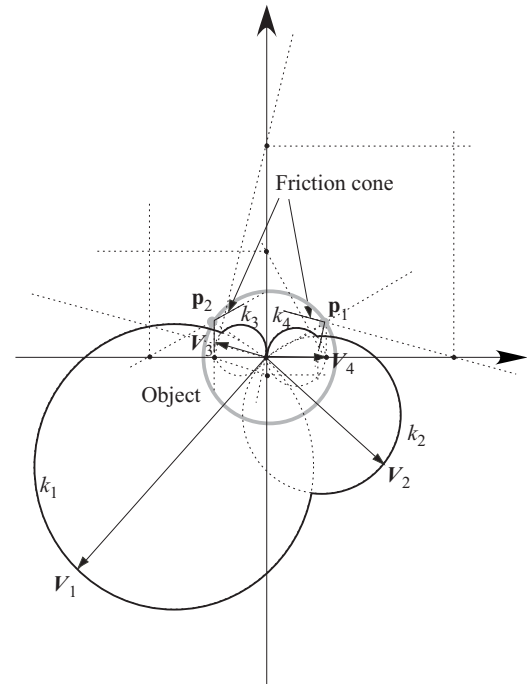
(a) Manual draw.
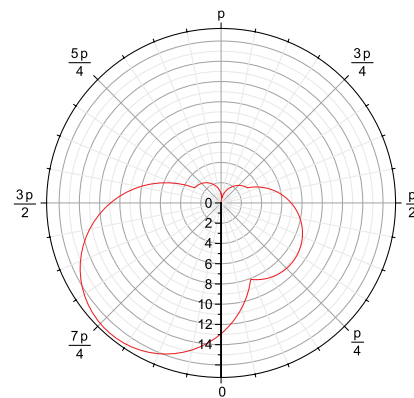
(b) Computer plot.

Fig. 6. (Colour online) Minimum internal force for grasping a circular object. (a) Manual draw; (b) computer plot.

force. The relative magnitude of the internal forces can be illustrated in a polar coordinate system, where the orientation corresponds to the external force direction. The actual magnitude of the internal force is proportional to that of the external force as well as the scale of the grasped object. Therefore, our proposed method provides the normalized forces in the object coordinate system. The actual value is obtained using Eq. (17) on the basis of magnitude of the external force, distance between the two contact points, and a value from the graph, specifically, the distance from the origin to a point on the graph in the direction of the external force.

The outline of the diagram is almost completely determined by the location of two friction cones. To clarify, let us take a typical example where $0 < \phi_i < \pi/2$, i.e., the CoM of the object is inward with respect to the object's surface. First, note that the intersection point of the circles

Case (a)

Case (b)

Case (c)

Fig. 7. Several shapes of internal force diagram in rectangular object grasp.
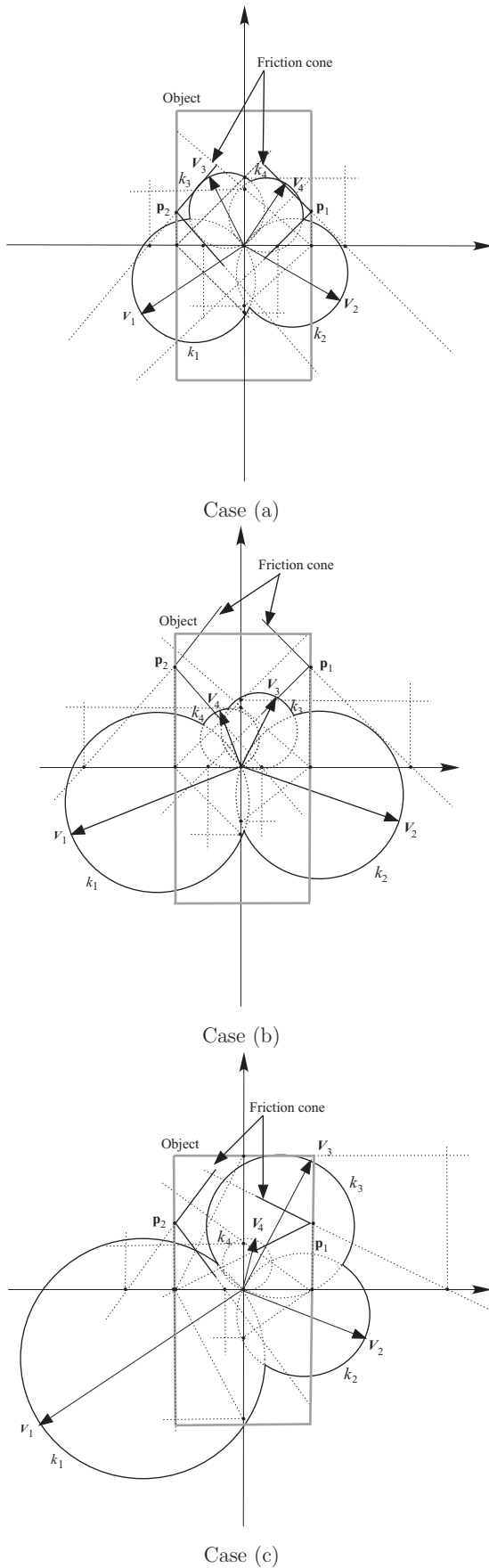
Table I. Parameters in rectangular object grasp.

	P_1	ϕ_1	μ_1	P_2	ϕ_2	μ_2
(a)	(2, 1)	$\pi/2$	1.0	(−2, 1)	$\pi/2$	1.2
(b)	(2, 3)	$\pi/2$	1.0	(−2, 3)	$\pi/2$	1.2
(c)	(2, 2)	$\pi/2$	0.5	(−2, 2)	$\pi/2$	1.4

and the intersection point of the lateral surfaces (edges in 2D grasp) of the friction cones are located on the same line, which also passes through the origin.[15] Next, we note that the contact point conditions $\pi/2 < \phi_i + \xi_i < \pi$ limit the vectors V_1 and V_2 within the region $y < 0$, and V_1 is located to the left of V_2. Regarding V_3 and V_4, the position of the point O_M is critical (see Fig. 8): If O_M is included in both friction cones, V_3 is in the region $x < 0$, while V_4 is in the region $x > 0$ (Fig. 8(a); Figs. 6 and 7(a) correspond to this case); if O_M is excluded from both friction cones, V_3 is in the region $x > 0$, while V_4 is in the region $x < 0$ (Fig. 8(b) whose example is Fig. 7(b)); otherwise, both V_3 and V_4 are in the same region $x > 0$ or $x < 0$ (Fig. 8(c) demonstrated by Figs. 5, 7(c), and 8(d)). Several cases should be considered for generalizing such diagram characteristics; however, we leave this for future study.

Now returning to consider the problem of determining the object orientation, recall that the diagram that we proposed in Section 3.1, i.e., the internal force diagram, represents forces in the object coordinate frame. Thus, if we set the magnitude of the external force as the weight of object and direction of the external force as downward (and the object orientation changes), then the result demonstrates the necessary internal force for this object orientation. If the internal force is set to be greater than the largest value of $|V_n|$, ($n = 1, 2, 3, 4$), the object is always stably grasped without slipping for any object orientation. This value is critical for creating a robust grasp.

6. Conclusion

In this paper, we have proposed a method to graphically express the minimum internal force required to grasp a 2D object with two points under external forces. A polar coordinate system is introduced: The orientation in the polar coordinate system represents the external force direction, while the distance from the origin represents the magnitude of the internal force required to resist the external force exerted in the corresponding direction. Based on the friction cone configuration, i.e., position, orientation, and apex angle, the diagram is manually drawn using only a ruler and compass. The validity of the manual drawing method has been confirmed by comparing it with computer-generated plots. The internal force diagram allows someone to visually understand the necessary internal force that depends on the direction of the external force, and whether the direction is easy or difficult for grasping, and how much internal force is required to provide a robust grasp. Such an understanding is useful and important for robot design. Extension of this method to 3D grasping will be studied in future.
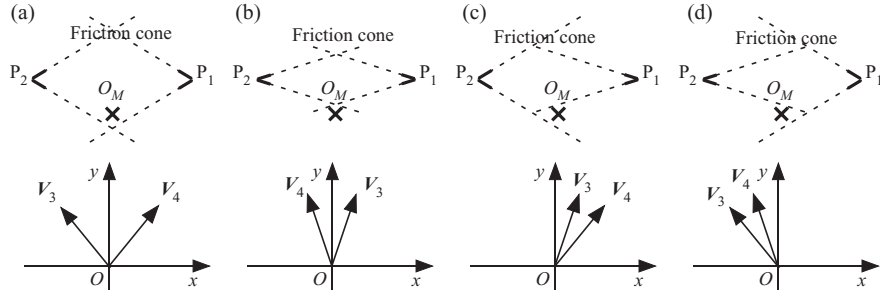
Fig. 8. Direction of V_3 and V_4 that depends on the spatial relation between friction cones and O_M.

Appendix

Relation between F_{int} and k

Let the element of $\boldsymbol{F}_N$ in Eq. (15) is

$$\boldsymbol{F}_N = [\, f_{N1} \ f_{N2} \ f_{N3} \ f_{N3} \,]^T. \tag{A1}$$

Then, the component orthogonal to $\boldsymbol{F}_T$ is written by $k\boldsymbol{F}_N = [\, kf_{N1} \ kf_{N2} \ kf_{N3} \ kf_{N3} \,]^T$, thus the magnitude of the internal force F_{int} becomes

$$F_{int} = k\sqrt{f_{N1}^2 + f_{N2}^2} = k\sqrt{f_{N3}^2 + f_{N4}^2}. \tag{A2}$$

Substituting f_{N1}, f_{N2}, f_{N3}, and f_{N4} by the each element of Eq. (15), we can obtain

$$F_{int} = k \cdot \frac{F_e}{x_1 + x_2}\sqrt{s^2 + c^2} = k \cdot \frac{F_e}{x_1 + x_2}, \tag{A3}$$

i.e., relation (17).

Proof of $\overline{O_M X_n} = -S_n$ and $\overline{OY_n} = -C_n$

Here, the case $n = 1$ is shown since the others are the same as this case. See Fig. 4(a). Notice that angles marked by double curved lines in Fig. 4(a) have the same amount, and let it be γ. Using this γ, we can describe $\overline{P_{1x}X_1}$ and $\overline{OY_1}$ as

$$\overline{P_{1x}X_1} = \overline{P_1 P_{1x}} \tan\gamma, \tag{A4}$$

$$\overline{OY_1} = \overline{OP_{2x}} \tan\gamma. \tag{A5}$$

Here, note that $\gamma = \pi - (\phi_1 + \xi_1)$, so

$$\tan\gamma = \tan(\pi - (\phi_1 + \xi_1)) = -\tan(\phi_1 + \xi_1). \tag{A6}$$

Thus, we obtain

$$\begin{aligned}
\overline{O_M X_1} &= \overline{O_M P_{1x}} + \overline{P_{1x}X_1} \\
&= \frac{x_1 + x_2}{2} + \overline{P_1 P_{1x}} \tan\gamma \\
&= \frac{x_1 + x_2}{2} + y \cdot (-\tan(\phi_1 + \xi_1)) = -S_1,
\end{aligned} \tag{A7}$$

$$\begin{aligned}
\overline{OY_1} &= \overline{OP_{2x}} \tan\gamma \\
&= x_2 \cdot (-\tan(\phi_1 + \xi_1)) = -C_1.
\end{aligned} \tag{A8}$$

References

1. V.-D. Nguyen, "Constructing force closure grasp," *Int. J. Robot. Res.* **7**(3), 3–16 (1988).
2. A. Bicchi, "On the closure properties of robotic grasping," *Int. J. Robot. Res.* **14**(4), 319 (1995).
3. X. Markenscoff and C. Papadimitriou, "Optimal grip of a polygon," *Int. J. Robot. Res.* **8**(2), 17–29 (1989).
4. B. Mirtich and J. Canny, "Easily Computable Optimum Grasps in 2-D and 3-D," **In**: *Proceedings of the IEEE International Conference on Robotics and Automation (ICRA'94)*, San Diego, CA, USA (May 8–13, 1994) pp. 739–747.
5. L. Mangialardi, G. Mantriota and A. Trentadue, "A three-dimensional criterion for the determination of optimal grip points," *Robot. Comput.-Integr. Manuf.* **12**(2), 157–167 (1996).
6. Y. Yong, K. Takeuchi and T. Yoshikawa, "Optimization of Robot Hand Power Grasps," **In**: *Proceedings of the IEEE International Conference on Robotics and Automation (ICRA'98)*, Leuven, Belgium, vol. 4 (May 1998) pp. 3341–3347.
7. T. Watanabe and T. Yoshikawa, "Optimization of Grasping by Using a Required External Force Set," **In**: *Proceedings of the IEEE International Conference on Robotics and Automation (ICRA 2003)*, (Sep. 14–19, 2003) pp. 1127–1132.
8. F.-T. Cheng and D. E. Orin, "Efficient algorithm for optimal force distribution – the compact-dual lp method," *IEEE Trans. Robot. Autom.* **6**(2), 178–187 (1990).
9. Y.-H. Liu, "Qualitative test and force optimization of 3-D frictional form-closure grasps using linear programming," *IEEE Trans. Robot. Autom.* **15**(1), 163–173 (1999).
10. D. Ding, Y.-H. Liu, M. Y. Wang and S. Wang, "Automatic selection of fixturing surfaces and fixturing points for polyhedral workpieces," *IEEE Trans. Robot. Autom.* **17**(6), 833–841 (2001).
11. E. A. Al-Gallaf, Multi-fingered robot hand optimal task force distribution neural inverse kinematics approach," *Robot. Auton. Syst.* **54**, 34–51 (2006).
12. V. N. Dubey, R. M. Crowder and P. H. Chappell, "Optimal object grasp using tactile sensors and fuzzy logic," *Robotica* **17**, 685–693 (1999).
13. S. Ito, Y. Mizukoshi, K. Ishihara and M. Sasaki, "Optimal Direction of Grasped Object Minimizing Contact Forces," **In**: *Proceedings of the 2006 IEEE/RSJ International Conference on Intelligent Robots and Systems* Beijing, China (Oct. 9–15, 2006) pp. 1588–1593.
14. S. Ito, Y. Mizukosi and M. Sasaki, "Numerical Analysis for Optimal Posture of Circular Object Grasped with Frictions," *Proceedings of the 2007 IEEE/RSJ International Conference on Intelligent Robots and Systems* (2007).
15. S. Ito, S. Takeuchi and M. Sasaki, "Object orientation in two dimensional grasp with friction towards minimization of gripping power," *Biol. Cybern.* **101**(3), 215–226 (2009).
16. X.-Y. Zhang, Y. Nakamura, K. Goda and K. Yoshimoto, "Robustness of Power grasp," **In**: *Proceedings of the IEEE International Conference on Robotics and Automation (ICRA'94)*, San Diego, CA, USA, vol. 4, (May 1994) pp. 2828–2835.
17. Y. Nakamura and S. Kurushima, "Computation of marginal external force space of power grasp using polyhedral convex set theory," *J. Robot. Soc. Japan* **15**(5), 728–735 (1997).